Journal of Integrative Agriculture 2026, 25(3): 1020–1034

Available online at ScienceDirect

Journal of Integrative Agriculture



RESEARCH ARTICLE

StCOMT1 enhances potato resistance to *Fusarium sporotrichioides* by regulating coumarin-related substance accumulation and the ROS system

Jiaqi Wang[1, 2*], Biao Zhao[1, 2*], Dan Liu[1], Fumeng He[1], Chong Du[1], Yunzhu Che[1], Zengli Zhang[1], Xu Feng[1], Xue Wang[3] ,Yingnan Wang[1#], Fenglan Li[1, 2, 3#]

[1] *College of Life Sciences, Northeast Agricultural University, Harbin 150030, China*
[2] *Heilongjiang High Quality Agricultural Functional Microbial Agent Engineering and Technology Research Centre, Harbin 150030, China*
[3] *Heilongjiang Green Food Science Research Institute, Harbin 150028, China*

Highlights

- Overexpression of *StCOMT1* enhances potato resistance to *Fusarium sporotrichioides*.
- *StCOMT1* overexpression leads to a reduction in reactive oxygen species (ROS) accumulation during pathogen infection.
- *StCOMT1* overexpression promotes the accumulation of coumarin-related compounds in potato.

Abstract

Caffeic acid-*O*-methyltransferase (COMT) is a crucial enzyme in the phenylpropanoid metabolic pathway, with significant roles in both the lignin and coumarin pathways. The function of *COMT* in plant disease resistance has been demonstrated in several species. Our research identified the potato *COMT* gene family on a genome-wide scale and *StCOMT1* as a candidate gene for enhancing potato disease resistance under DON induction through phylogenetic analyses combined with previously identified metabolic differences and weighted gene co-expression network analysis (WGCNA) results. In order to better understand the function of *StCOMT1*, heterologous expression and overexpression assays were conducted. StCOMT1 is localized in chloroplasts and was found to catalyze the methylation of substrates to produce ferulic acid and melatonin *in vitro*. Physiological parameters showed that, compared with wild-type potato plants, *StCOMT1*-overexpressing plants infected with *Fusarium sporotrichioides* exhibited smaller lesion areas and lower reactive oxygen species (ROS) levels. High-performance liquid chromatography (HPLC) and RT-qPCR analyses revealed organ-specific accumulation of coumarin-related compounds and organ-specific expression of their corresponding genes in *StCOMT1*-overexpressing plants post-inoculation. The results indicate that *StCOMT1* overexpression in potatoes enhanced resistance to *F. sporotrichioides* by enhancing reactive oxygen species clearance and promoting organ-specific accumulation of coumarin-related compounds.

Keywords: potato, *COMT* gene, overexpression, disease resistance, ROS scavenging

1. Introduction

The potato (*Solanum tuberosum* L.) is a crucial non-cereal food crop, providing more calories per unit weight than cereal crops. Fresh and processed potatoes are popular due to their high carbohydrate content, as well as their abundance of vitamin C and other nutrients (Camire *et al.* 2009; Stokstad 2019). Potato dry rot (PDR) caused by *Fusarium* species infection of potato tubers during storage can cause 6.25–25% tuber loss every year (Xue *et al.* 2013). In particular, when the tubers are injured, the infection rate can reach up to 60% (Fan *et al.* 2021), resulting in huge economic losses. These *Fusarium* species infect potato tubers through wounds in the potato epidermis, causing gradual dehydration that can lead to complete rot, which significantly affects potato quality and

Received 11 November 2024; Received in revised form 17 January 2025; Accepted 19 May 2025; Available online 15 November 2025
Jiaqi Wang, E-mail: wjq13941677600@163.com; Biao Zhao, E-mail: zhaob35@outlook.com; #Correspondence Yingnan Wang, E-mail: yingnan1027@foxmail.com; Fenglan Li, E-mail: lifenglan@neau.edu.cn

© 2026 CAAS. Publishing services by Elsevier B.V. on behalf of KeAi Communications Co. Ltd. This is an open access article under the CC BY-NC-ND license (http://creativecommons.org/licenses/by-nc-nd/4.0/). Peer review under responsibility of Editorial Board of *Journal of Integrative Agriculture*.
doi: 10.1016/j.jia.2025.11.021

sales. Annual losses of frozen potatoes due to *Fusarium* have been estimated to be as high as 25–60% (Tiwari *et al.* 2023), and in north-eastern China, common *Fusarium* species include *F. sporotrichioides*, *F. sambucinum*, and *F. culmorum* (Xue *et al.* 2023). *Fusarium* produce mycotoxins, including T-2, DON (deoxynivalenol), and ZEN (zearalenone), during infestation. These mycotoxins pose a potential threat to human health (Morimura *et al.* 2020).

DON is produced when *F. sambucinum*, *F. culmorum*, and other *Fusarium* species infect cereal crops and potatoes (Xue *et al.* 2023; Zöngür 2024). Additionally, it has been shown to act as an elicitor, stimulating plant immune responses at low concentrations (Doppler *et al.* 2019; Zhao *et al.* 2020; Wei *et al.* 2023). Elicitors can activate plant immunity and trigger plant defense responses. Various fungal elicitor effects have been demonstrated, such as the protein elicitor PevD1 secreted by *Verticillium dahliae*, which induces increased synthesis of salicylic acid (SA) and lignin, enhancing disease resistance in *Arabidopsis thaliana* (Li *et al.* 2022). The elicitor PeaT1 isolated from *Alternaria tenuissma* can improve the activity of protective enzymes in tobacco and induce the accumulation of SA and jasmonic acid (JA) in wheat to participate in physical defense (Li *et al.* 2019). *TaMetRS* genes, activated by DON treatment in wheat resulted in significant resistance to *F. graminearum* (Zuo *et al.* 2016). Our previous study also showed that low concentrations of DON treatment could induce systemic acquired resistance in potato (Zhao *et al.* 2020; Wei *et al.* 2023). Under the treatment of 5 ng mL^{-1} DON, transcriptome data analysis revealed that differentially expressed genes (DEGs) were significantly enriched in the pathways of phenylpropanoid and flavonoid metabolism. The secondary metabolic pathway of coumarin within phenylpropanoid metabolism was crucial in the immune response (Zhao *et al.* 2023). Coumarin analogues are released after cell damage and have primarily defensive functions. Coumarin derivatives inhibit bacterial diseases in plants (Feng *et al.* 2022), while coumarin scopoletin inhibits the activity of the Asian rust fungus *Phakopsora pachyrhizi*, protecting soybeans and reducing the damage caused by disease infestation (Beyer *et al.* 2019).

Caffeic acid *O*-methyltransferases (COMTs) play essential roles in the phenylpropanoid metabolic pathway and coumarin metabolism. They also have significant functions in both lignin and flavonoid biosynthesis (Liu *et al.* 2021). COMT catalyzes the generation of melatonin from N-acetyl-5-hydroxytryptamine and also the methylation of caffeic acid to produce ferulic acid (Liang *et al.* 2022). There is evidence that COMT might have evolved from N-acetylserotonin methyltransferases (ASMT) through gene duplication and subsequent divergence (Zhao D *et al.* 2021). COMT has a more conserved substrate-binding site and a more open protein conformation than ASMT. As a result, it has a higher activity that produces more melatonin for plants to acclimate to stressful land environments (Zhao D *et al.* 2021). Deletion of *COMT* results in altered lignin monomer composition ratios and content (Daly *et al.* 2018; Saluja *et al.* 2020). The *MsCOMT* gene from *Miscanthus sinensis* was down-regulated in tobacco, resulting in a decrease in the expression of ascorbate peroxidase in transgenic tobacco. Additionally, overexpression of the antisense *MsCOMT* gene in tobacco caused a reduction in PAL expression, lignin levels and possibly soluble phenolics (Seong *et al.* 2012). The role of *COMT* genes in wheat may be related to stem rigidity and lodging resistance (Ma *et al.* 2002). Wheat overexpressing the *TaCOMT-3D* gene can enhance stem mechanical strength by promoting lignin (particularly syringyl monolignol) accumulation, thereby enhancing resistance to sharp eyespot (Wang M *et al.* 2018). A *COMT* loss-of-function mutation in sorghum reduces butyl lignin subunits, decreases lateral root density, and increases the transcript abundance of genes involved in (a)biotic stress responses (Saluja *et al.* 2020). Overexpression of *COMT* in watermelon increased melatonin content and enhanced the tolerance of watermelon to abiotic stress (Chang *et al.* 2021). L-Methionine treatment can cause differential expression of phenylpropanoid pathway genes, such as COMT. It also leads to the up-regulation of metabolites, such as trans-ferulic acid, which can improve antioxidant capacity and trigger immune responses to enhance the resistance of winter jujube to black rot (Yang *et al.* 2024).

In this study, we analyzed the *COMT* gene family in 'Atlantic' potatoes and combined it with DEG and WGCNA analysis. A significant upregulation of the coumarin biosynthesis key gene *StCOMT1* under DON induction was observed. To further explore the function of *StCOMT1* in potato resistance, *F. sporotrichioides* infection assays were conducted on 'Atlantic' potatoes overexpressing the *StCOMT1* gene. Disease resistance physiological indicators and the content of four secondary metabolites, including caffeic acid, ferulic acid, melatonin, and scopoletin, were measured in the *StCOMT1*-overexpression lines and the wild-type plants. It was found that *StCOMT1*-overexpressing plants exhibited stronger resistance to *F. sporotrichioides* compared to wild-type plants. Overexpression of *StCOMT1* effectively reduced reactive oxygen species (ROS) oxidative damage and increased the accumulation of coumarin-related compounds.

2. Materials and methods

2.1. Identification of candidate genes of the *StCOMT* family in potato

***COMT* gene identification** The genome data of 'Atlantic' potato was downloaded from a database (https://datadryad.org/stash/dataset/doi:10.5061/dryad.3n5tb2rhw). The Hidden Markov model (HMM) number for the Methyltransf_2 structural domain of the *COMT* gene is PF00891 (http://pfam.xfam.org). The hmmsearch program from the HMMER software was utilised to search for all genes containing the PF00891 model in the 'Atlantic' genome protein file. Protein sequences of genes with an e-value of less than $1e^{-20}$ were extracted to construct a new HMM model of specific conserved structural domains. This new HMM model was then used to repeat the search for members of the potato protein gene family and screen for e-values less than 0.01. The genes were annotated and analysed using EggNOG (http://eggnog5.embl.de/). The obtained genes were further screened, and those clustered as *COMT* gene family

members had their protein sequences extracted.

Chromosome localization and phylogenetic analysis All *COMT* annotations and chromosomal loci in the 'Atlantic' potato annotation file were extracted, and *Arabidopsis* and *Solanum lycopersicum* COMT protein sequences were obtained according to existing reports (Letunic and Bork 2007; Liu *et al.* 2021; Liang *et al.* 2022). Chromosome mapping of *StCOMT* loci in potatoes was performed using TBtools and the online tool MapGene2Chrom web v2 (Chao *et al.* 2015). Phylogenetic trees were constructed using MEGA 11 software with the maximum likelihood (Pasare *et al.* 2013) method for evolutionary tree construction. The Bootstrap method was set to 1,000 replicates and other default parameters (Zuckerkandl and Pauling 1965) were used. Branch lengths were labeled to infer evolutionary distances in the phylogenetic trees.

Analysis of exon and intron structure, motifs, and physicochemical properties TBtools was used to visualize the results of protein conserved domains (Chen *et al.* 2020). According to the motif prediction results obtained from the online website MEME(http://meme-suite.org/tools/meme), the motif result map of StCOMTs was drawn using TBtools. NCBI-CDD (http://www.ncbi.nlm.nih.gov/cdd) was used for structural domain prediction and visualized with TBtools. ProtParam (https://web.expasy.org/protparam/) was used to predict the basic physical and chemical properties of the proteins.

Gene duplication and syntenic analysis The Simple Ka/Ks Calculator (NG) of TBtools (Chen *et al.* 2020) was used to calculate the Ka/Ks ratio for tandemly duplicated genes and to analyze the evolutionary selection pressure on the *StCOMT* gene family. Gene duplication events were analyzed using Multiple Collinear Scanning Toolkits (MCScanX) with default parameter values (Wang *et al.* 2012).

Transcriptome data analysis and WGCNA analysis The specific methods for DON treatment of potato tubers and the transcriptome and metabolome analyses are described in prior report (Zhao *et al.* 2023). DEGs, WGCNA module genes and *StCOMT* family genes were collected to draw a Venn diagram. A gene expression heatmap was generated using the heatmap package in R, based on the expression levels (Transcripts Per Million, TPM) of genes common to all sets in the Venn diagram at distinct time points during DON treatment. The raw sequencing data of potato tubers transcriptome under DON treatment have been uploaded to the NCBI SRA sequence read file PRJNA943451 project (https://www.ncbi.nlm.nih.gov/sra/?term=%20PRJNA943451).

2.2. *StCOMT1* gene cloning and subcellular localization

The selected gene *Soltu.Atl.03_2G015140* was renamed as *StCOMT1*. The gene sequence was downloaded from the relevant database, and the primers *STCOMT1*-F/R (Appendix A) were designed using SnapGene v6.0.2. Total RNA was extracted from 'Atlantic' potato tubers using a plant RNA extraction kit (Beijing Tiangen Biochemical Co., Ltd.) and tested for integrity. Using primer *StCOMT1*-F/R, the *StCOMT1* gene was cloned from the reverse-transcribed cDNA as a template and ligated into the pEASY-T3 vector. The *StCOMT1* open reading frame (ORF) sequence, without the stop codon, was cloned into the pCAMBIA2300-eGFP vector using the homologous recombination primers T_*StCOMT1*_F/R (Appendix A). *Agrobacterium tumefaciens* LBA4404 containing pCambia2300-*StCOMT1*-eGFP was injected into 4-wk-old *Nicotiana benthamiana* leaves. After 48 h, the injected tobacco leaves were harvested, and the fluorescence signals were observed using an ultra-high resolution laser confocal microscope (LSM800, Zeiss, Germany) with an excitation wavelength of 488 nm for GFP and 640 nm for chloroplast fluorescence signals.

2.3. Prediction of StCOMT1 protein structure and molecular docking

The StCOMT1 protein sequence was subjected to homology modeling using SWISS-MODEL (https://swissmodel.expasy.org/). The resulting model was then overlaid and aligned with similar protein structures using Chimera. Protein structure prediction was performed using the monomer model in AlphaFold v2.3.2 with default parameters. The following database versions were used: UniProt and UniRef90 (2023-03-01), PDB_MMCIF and PDB_SEQRES (2023-03-03). All other database versions used were the default versions. The StCOMT1 protein structure and the structures of caffeic acid and N-acetyl-5-hydroxytryptamine were obtained from the Protein Data Bank (http://www.rcsb.org/pdb) and PubChem (https://pubchem.ncbi.nlm.nih.gov/). Protein binding to compounds was simulated using AutoDock Vina (version 1.1.2). Visualization of molecular docking was performed using PyMOL software (version 2.3.4).

2.4. Expression of *StCOMT1* in a heterologous system

The prokaryotic expression vector pET32a was employed for heterologous expression. Subsequently, the pET32a-*StCOMT1* recombinant expression vector was digested with *Bam*HI and *Xho*I, followed by transformation into the host bacteria. The primers *StCOMT1_Bam*HI_32a-F and *StCOMT1_Xho*I_32a-R are shown in Appendix A. BL21 (DE3) cells containing either the pET32a-StCOMT1 vector or the empty vector were cultured and induced with Isopropyl β-D-Thiogalactopyranoside (IPTG) for 8 h. The His-tagged Protein Purification Kit (P2226, Beyotime Biotechnology, Shanghai, China) was used for protein purification, and the proteins were concentrated using Millipore Ultra centrifuge filter tubes. The 10 μg mL^{-1} target protein was mixed with 200 μmol L^{-1} caffeic acid and N-acetyl-5-hydroxytryptamine as substrates, along with 1 mmol L^{-1} SAM, 1 mmol L^{-1} dithiothreitol, and 200 mmol L^{-1} Tris-HCl buffer (pH 7.0) to form a 10 mL system. After a 20-min reaction, concentrated sulfuric acid was added to terminate the reaction, and the reaction products were analyzed by high-performance liquid chromatography (HPLC).

2.5. Preparation of construct and potato transformation

The *Bam*HI and *Xba*I restriction enzyme cutting sites were inserted using the primers *StCOMT*1_pBI121F/R (Appendix A). Then, a double enzyme digestion on both the pBI121

plasmid and the T3-*StCOMT1* plasmid was performed. The digested product *Xba*I-*StCOMT1*-*Bam*HI was ligated with the double-digested pBI121 expression vector by T4 ligase and transformed into pBI121. The recombinant vector, named pBI121-*StCOMT1*, was transferred into *A. tumefaciens* LBA4404 for subsequent infection.

The 'Atlantic' potato micro-tubers were provided by the Agricultural Academy of Heilongjiang Province, China. The method for genetic transformation was conducted as previously described (Ma *et al.* 2022). Potato tubers were sterilized, peeled and cut into 2-cm-thick sections, and then infected with *A. tumefaciens* LBA4404 containing the pBI121-*StCOMT1* plasmid. The potato pieces were transferred to co-culture medium: MS+1.5 mg L^{-1} indole acetic acid (IAA) +3.0 mg L^{-1} zeatin (ZT), pH 5.8, and cultured in the dark for 2 d. Subsequently, the explants were transferred to differentiation media: MS+1.5 mg L^{-1} IAA+3.0 mg L^{-1} ZT+100 mg L^{-1} kanamycin+50 mg L^{-1} cefotaxime, pH 5.8, and cultured in a tissue culture chamber at 25°C with a 16-h light/8-h dark cycle. DNA was extracted from both transgenic and wild-type plants, and PCR amplification was performed using the *GUS* gene-specific primer pair *GUS*-F/R (Appendix A) and a direct amplification kit. The amplification products were analyzed by agarose gel electrophoresis, and the plants with correct bands were propagated using tissue cultured (Bruce and Shoup Rupp 2019).

2.6. Determination of disease resistance in *F. sporotrichioides*-infected transgenic potatoes

***Fusarium sporotrichioides* inoculation and lesion detection** Tissue-cultured seedlings of *StCOMT1*-overexpressing potato lines OE1 and OE2, and wild type 'Atlantic' potato (WT) at 3–4 wk of age were transplanted simultaneously into 17 cm diameter plastic pots containing a 1:1 (v/v) mixture of vermiculite and nutrient soil under 16 h light, 8 h dark, 3,000 lx light, and temperature of 20–28°C. *Fusarium sporotrichioides* (stored and provided by our laboratory) infection was performed by *in vitro* inoculation of leaves. The third fully expanded compound leaf from the top of six-wk-old healthy overexpressing and wild-type potato plants was used for inoculation in subsequent experiments. During inoculation, 10 μL *F. sporotrichioides* conidia suspension (1×10^5 CFU mL^{-1}) (Xue *et al.* 2017) was dripped onto the area near the vein on the dorsal side of the leaf using a pipettor to avoid damage to the leaf. Sterile filter paper saturated with sterile water was placed on the culture dish, and the petioles were wrapped with infiltrated medical absorbent cotton. The culture dish was incubated at 25°C and light for 16 h d^{-1}. Leaves of WT, OE1, and OE2 plants inoculated at 0, 1, 3, 5, and 7 days after inoculation (dai) were collected for phenotypic and physiological analyses. The plaque diameter was measured using a vernier caliper.

Measurement of physiological and biochemical indicators The WT, OE1 and OE2 leaves exposed to *F. sporotrichioides* at 1, 3, 5 and 7 dai were stained with trypan blue (van Wees 2008). Leaves of WT, OE1 and OE2 plants exposed to *F. sporotrichioides* at 0, 1, 3, 5 and 7 dai were collected for the subsequent detection. The active site of peroxidase in the cells was detected by diaminobenzidine (DAB) staining (Daudi and O'Brien 2012). Hydrogen peroxide (H_2O_2) content, superoxide anion ($O_2^{-}\cdot$) content, and superoxide dismutase (SOD), catalase (CAT), and peroxidase (POD) activities were determined according to the instructions provided in an assay kit (Suzhou Keming Biotechnology Co., Ltd., China) (Liu *et al.* 2022). All experiments were performed with three biological replicates. Data were analyzed using GraphPad Prism 9.

Morphological observations of mycelium during *F. sporotrichioides* infection Six-wk-old leaves that had been treated according to the previous method of *in vitro* inoculation for 3 d and *F. sporotrichioides* that had been cultured in petri dishes for 3 d were used as the test materials. Infected leaves and fungal cultures were then fixed in glutaraldehyde at pH 6.8 and 4°C for 1.5 h, rinsed twice in pH 6.8 phosphate buffer for 10 min each, dehydrated in 50, 70, and 90% ethanol, and finally replaced with 100% ethanol: tert-butanol (1:1) for 15 min, and pure tert-butanol twice, 15 min each. The samples were then dried in a freeze-dry desiccator. After drying, the samples were placed on the scanning electron microscope (SEM) sample stage using conductive tape. After coating a layer of metal film with a thickness of 100–150 angstroms on the surface of the samples using an ion-sputtering coater, the morphology of hyphae was observed by SEM.

2.7. Detection of coumarin and coumarin-related compounds in *StCOMT1* Overexpression potato lines

WT, OE1 and OE2 plant tubers, leaves, and stems were selected to prepare temporary mounts. The coumarin compounds were indicated using a fluorescence microscope, excited with blue autofluorescence at an excitation wavelength of 353 nm. OE1, OE2 and WT potato plants were inoculated with 20 μL *F. sporotrichioides* suspension of conidia (1×10^5 CFU mL^{-1}), and the roots, stems, leaves, and tubers were selected as samples 3 dai. The contents of caffeic acid, ferulic acid, melatonin, and scopoletin in each sample were detected by HPLC. The standard samples were purchased from Shanghai Yuanye Bio-Technology Co., Ltd. Each sample was weighed to be 1.0 g, and 5.0 mL of 75% methanol were added. The mixture was subjected to ultrasonic treatment for 20 min. Then, it was centrifuged at 4,500 r min^{-1} for 30 min. Subsequently, 250 μL of the supernatant was filtered through a 0.45 μm filter membrane, and the filtrate was collected for analysis. The standard products were directly dissolved in 75% methanol. The liquid phase conditions were as follows. The Agilent C18 polar column (4.6 mm×250 mm, 5 μm) was used with a mobile phase consisting of acetonitrile (A) and 0.1% aqueous phosphoric acid (B) at a flow rate of 1 mL min^{-1}. The column temperature was maintained at 30°C, and the injection volume was 10 μL. Detection was performed at wavelengths of 330 and 225 nm using gradient elution. The gradient elution program was as follows: 0–15 min, 10% A; 15–35 min, 15% A; 35–40 min, 20% A; 40–45 min, 25% A; 45–50 min, 10% A.

2.8. Expression analysis using RT-qPCR

The expression levels of *StCOMT1* in various parts of

WT and overexpression plants and the expression levels of coumarin-related genes in various parts of the plants after *F. sporotrichioides* inoculation were detected by qRT-PCR. The LineGene 9620 Real-Time PCR System from BIOER was used, and *β-actin* was used as the reference gene. The genes analyzed were *PAL*, *C4H*, *4CL*, *F6′H*, *COSY*, *C3′H*, *HCT*, *CCoAOMT*, *UGT*, *S8H*, *CYP82C4*, and *BGLU*, and their respective primers are shown in Appendix B. The Total RNA Rapid Extraction Kit (ER501-01, TransGen Biotech, Beijing, China) was used to extract total RNA from each treated sample. The extracted RNA was then reverse transcribed to cDNA using TransScript® One-Step gDNA Removal and cDNA Synthesis SuperMix (AT311, TransGen Biotech, Beijing). The ChamQ Universal SYBR qPCR Master Mix (Q711, NJ, Vazyme) Kit was used for RT-qPCR reactions. The data obtained from three independent replicates were analyzed using the $2^{-\Delta\Delta Ct}$ method (Lu *et al.* 2022).

3. Results

3.1. Phylogenetic analysis of the *COMT* gene family in 'Atlantic' potato

We identified 123 members of the *StCOMT* gene family in the 'Atlantic' potato genome using the Pfam model and gene function annotation. We then predicted their protein physicochemical properties, as detailed in Appendix C. The 123 StCOMT proteins had amino acid residues ranging from 81 to 896, with protein molecular weights ranging from 8.86564 to 99.81227 kDa. The isoelectric points ranged from 4.73 to 9.49, indicating that most are acidic proteins (a total of 113). The aliphatic index ranged from 17.27 to 49.03, and 110 of them had an instability index of less than 40 and were stable proteins. The lipid index ranged from 84.39 to 125.06, while the hydrophilicity ranged from –0.259 to 0.552. Out of the total, 77 proteins were hydrophilic (with a hydrophilicity value less than 0).

The *StCOMT* gene family has major motifs, including VSHVGGDMFNSVPSADAILLK, VTVGGKER TEKEWAK LFKEAGFS, and SMAPFLLFELDPVL MNPWHYL SDWILSGEN. Members of the gene families that are grouped according to evolutionary relationships have similar gene structures. For example, *Soltu.Atl.06_1G016320*, *Soltu.Atl.06_4G022360*, *Soltu.Atl.06_1G016350*, and *Soltu.Atl.06_4G022390*, *Soltu.Atl.06_4G022370*, *Soltu.Atl.06_1G016330*, *Soltu.Atl.06_4G022380*, and *Soltu.Atl.06_1G016340* exhibit identical motif distribution, each containing eight identical motifs (Fig. 1-A). Analysis of gene structure revealed that the *StCOMT* gene family comprises exons ranging from 1 to 16. Members of the *StCOMT* gene family contain one or more Methyltransf_2 conserved structures. Additionally, many *StCOMT* genes, including *Soltu.Atl.10_2G003100* and *Soltu.Atl.10_3G001670*, *Soltu.Atl.10_4G001680*, *Soltu.Atl.10_1G002550*, *Soltu.Atl.10_4G001650*, *Soltu.Atl.10_2G003050*, and *Soltu.Atl.08_0G002670* also contain internal_repeat_1, RRM, HTH_IclR and other conserved structural domains (Fig. 1-B).

Tandem duplication is an important mechanism for expanding gene families (Cannon *et al.* 2004). The Ka/Ks values of all tandemly duplicated gene pairs in the *StCOMT* gene family were less than 1, indicating a negative selection effect (Appendix D). Segmental duplication events occurred on chromosomes 1, 2, 3, 5, 6, 9, 10, and 12. These events were concentrated on homologous chromosomes, with only two pairs of segmental duplication events occurring on non-homologous chromosomes (chr09_2 and chr06_4, and chr06_1) (Fig. 1-C). These results suggest that the *StCOMT* gene may have originated from gene duplication and that segmental duplication events are important drivers of *StCOMT* evolution and play an important role in the expansion of the *COMT* gene family in 'Atlantic' potato. *StCOMTs* were unevenly distributed across potato chromosomes, with 123 genes widely distributed on 36 chromosomes (Fig. 1-D). Chromosome 3 had the highest number of genes (36), while chromosomes 4 and 7 did not have any members of the *StCOMT* gene family.

3.2. Gene family and co-expression analysis predicts functional genes

Phylogenetic analysis revealed that the 123 *StCOMT* genes could be classified into four subfamilies. *StCOMT* I did not cluster with *Arabidopsis* and tomato in the same clade. *StCOMT* II may encode an N-acetylserotonin *O*-methyltransferase, which converts N-acetylserotonin to melatonin during melatonin synthesis and serotonin to 5-methoxytryptamine but does not possess caffeic acid *O*-methyltransferase activity. *StCOMT* III may encode nicotinic acid N-methyltransferase, which is involved in the formation of N-methylnicotinic acid ester. *StCOMT* IV may encode caffeic acid/5-hydroxyferulic acid *O*-methyltransferase, which possesses *O*-methyltransferase activity, S-adenosylmethionine-dependent methyltransferase activity, acetylserotonin *O*-methyltransferase activity, caffeic acid *O*-methyltransferase activity, lignocerol *O*-methyltransferase activity, and quercetin 3-*O*-methyltransferase activity (Fig. 2-A).

By combining DEGs in potato transcriptome induced by previous DON treatment, WGCNA (Zhao *et al.* 2023), and the phylogenetic tree, we have narrowed down the candidates of *COMT* genes that may play a key role in potato disease resistance following DON application. The WGCNA prediction module yielded 16 *StCOMT* genes (Fig. 2-B). Heatmaps were used to display the expression patterns of the genes at different time points (Fig. 2-C). It is noteworthy that *Soltu.Atl.03_2G015140* and *Soltu.Atl.03_1G017640* were significantly more highly expressed than other genes at 4, 12, and 48 h post-DON treatment. The gene sequences of *Soltu.Atl.03_2G015140* and *Soltu.Atl.03_1G017640* were identical. Therefore, we designated this gene sequence as *StCOMT1* that may be a key gene in coumarin synthesis.

3.3. *StCOMT1* is involved in the biosynthesis of ferulic acid and melatonin

To investigate the biological function of *StCOMT1* in the resistance of 'Atlantic' potatoes to dry rot disease, we cloned and heterologously expressed the *StCOMT1* gene. The cloned product was 1,092 bp in size (Appendix E), and sequence comparison revealed no mutation sites (Appendix F). The *StCOMT1* gene encodes a predicted hydrophilic

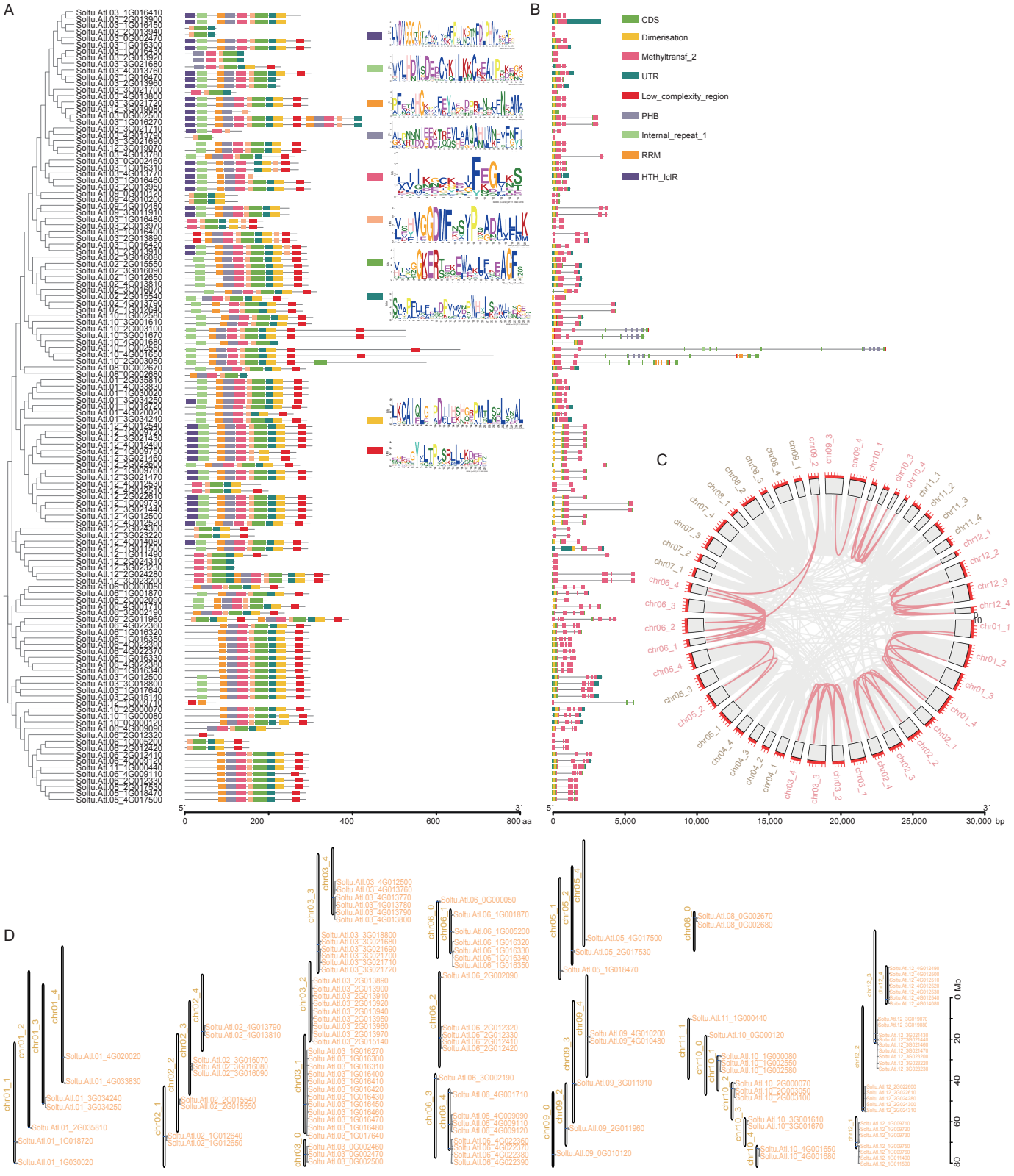


Fig. 1 The polygenetic relationship, motif analysis, gene structure, chromosomal location of *StCOMTs* and synteny analysis of *StCOMT* genes. A, the phylogenetic tree of *StCOMT* genes and motif distribution of StCOMTs proteins. B, structures of the *StCOMT* genes. C, synteny analysis of *StCOMT* genes in the potato genome. The gray lines indicate all synteny blocks in the potato genome, and the red lines indicate duplicated *StCOMT* gene pairs. D, the locations of *StCOMTs* on the chromosome.

acidic protein consisting of 363 amino acids, with a protein molecular weight of 39.6 kDa, an isoelectric point of 5.71, an instability index of 32.14, a lipid index of 86.53, and a hydrophilicity of –0.032 (Appendix C).

The StCOMT1 protein structure was predicted using the homology modeling approach, and it was observed that

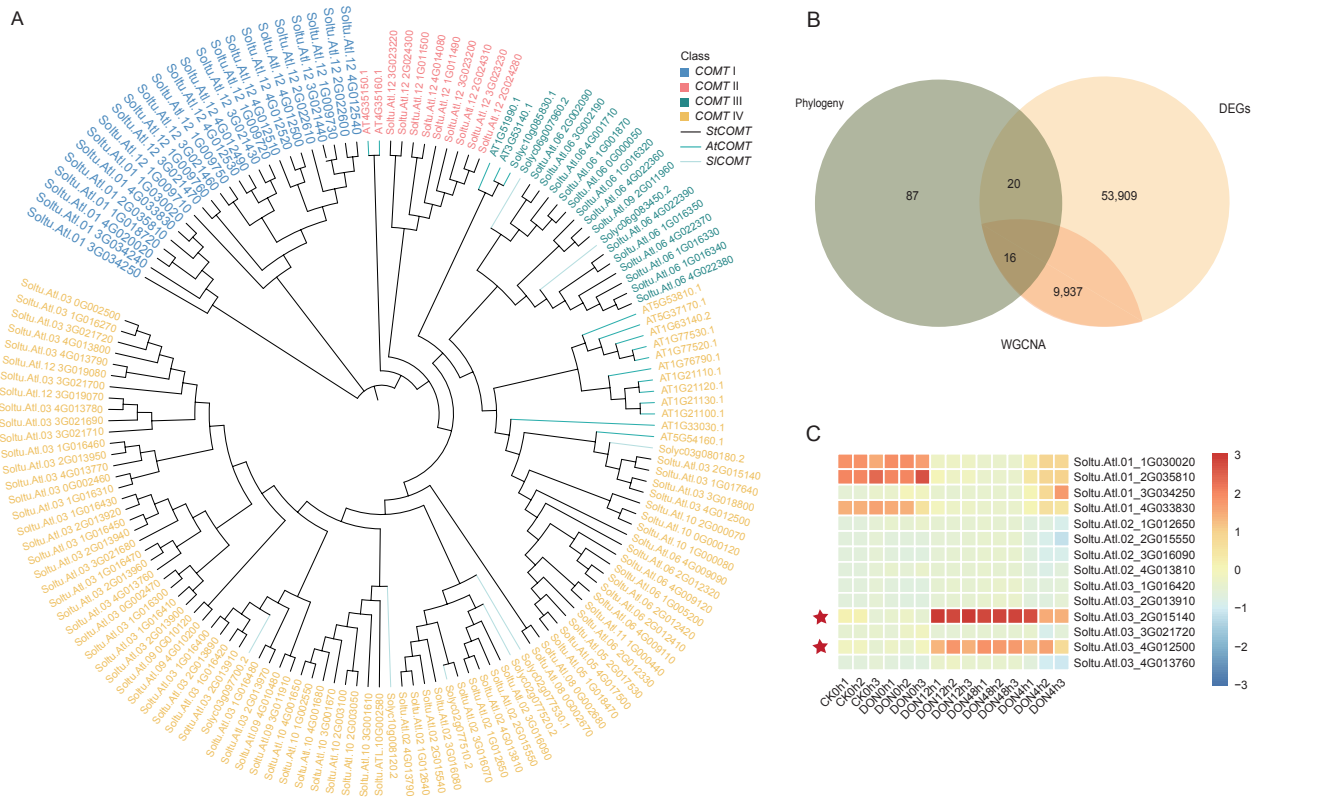


Fig. 2 *COMT*s in potato, *Arabidopsis*, and tomato with joint transcriptional analysis of key genes. A, the evolutionary relationship of *COMT*s in potato (St), *Arabidopsis thaliana* (At) and *Solanum lycopersicum* (Sl). B, differentially expressed genes (DEGs) obtained through transcriptome analysis, gene-weighted co-expression network analysis (WGCNA), and phylogenetic tree joint analysis. C, heatmap of the expression patterns of the 16 *StCOMT* genes over time.

the StCOMT1 protein contains a S-adenosylmethionine (SAM)-binding pocket along with a phenylpropanoid substrate pocket (Fig. 3-A). In the presence of StCOMT1, SAM is transferred to the caffeic acid 3-*O* position of the phenylpropanoid substrate molecule through hydrogen bonding of amino acids ALA-213, GLY-212, and THR-211 (Fig. 3-B). The binding mode of SAM to StCOMT1 with N-acetyl-5-hydroxytryptamine as a substrate is shown in Fig. 3-C. The reaction involves hydrogen bonding with key amino acids ASN-324 and ASP-270. To investigate the enzymatic activity of StCOMT1, we studied the expression and purification of the StCOMT-His fusion protein in an *E. coli* expression system. The purified protein was obtained after concentrating the His-tagged protein through nickel-column purification (Fig. 3-D). The function of StCOMT1 was verified *in vitro*. The standard product was analyzed by HPLC, and the enzyme activity was analyzed with N-acetyl-5-hydroxytryptamine and caffeic acid as substrates. The enzyme encoded by *StCOMT1* produces ferulic acid (P2) when caffeic acid (P1) is used as the substrate. The HPLC retention time of this product was 22.369 min, which was consistent with the retention time of the ferulic acid standard (21.869 min). When using N-acetyl-5-hydroxytryptamine (P3) as the receptor, the StCOMT1 converted it to melatonin (P4) with a retention time of 27.199 min, consistent with the melatonin standard (26.516 min). When using caffeic acid and N-acetyl-5-hydroxytryptamine as receptors, the StCOMT1 could convert both substrates. However, caffeic acid reduced ASMT activity and did not affect COMT activity (Fig. 3-E).

3.4. Subcellular localization and overexpression of *StCOMT1*

Fluorescence microscopy was used to observe green fluorescence throughout tobacco epidermal cells infected with Agrobacterium containing subcellularly localized vectors. The pCambia2300-eGFP expression vector caused green fluorescence throughout the cells, while the pCambia2300-*StCOMT1*-eGFP expression vector caused green fluorescence specifically in chloroplasts (Fig. 4-A). This suggests that StCOMT1 is localised in chloroplasts.

The potato variety ‘Atlantic’ was genetically transformed using the LBA4404-pBI121-*StCOMT1* expression vector *via* Agrobacterium-mediated transformation. Out of a total of 16 regenerated plants, six transgenic plants (named PS 1–6) were identified using the GUS reporter gene (Appendix G). The quantitative analysis of *StCOMT1* expression in transgenic potato leaves showed that the expression level of *StCOMT1* in PS1 and PS6 transgenic plants was significantly higher than that in WT plants (Fig. 4-B), which were named OE1 and OE2, respectively. The transgenic plants were propagated and transplanted into soil.

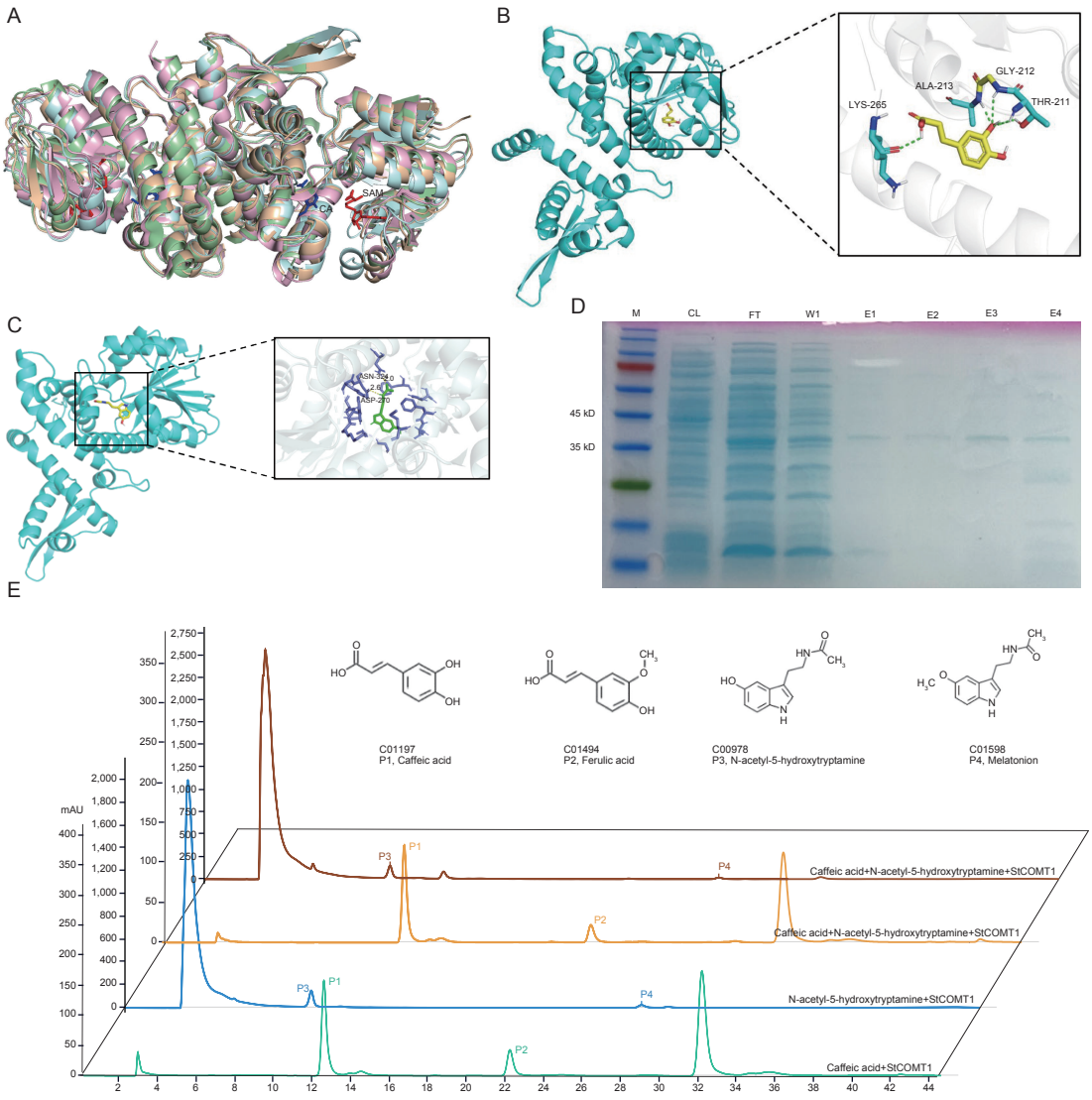


Fig. 3 StCOMT1 protein structure prediction and *in vitro* functional validation. A, 3D structure prediction of the StCOMT1 protein. B, molecular docking diagram of caffeic acid with StCOMT1. C, molecular docking diagram of N-acetyl-5-hydroxytryptamine with StCOMT1. D, purification results of StCOMT1 (M, marker; CL, cell lysate; FT, flow through; W1, wash 1; E1–E4, elution 1–4). E, protein catalytic activity analysis of StCOMT1 using N-acetyl-5-hydroxytryptamine and caffeic acid as substrates.

3.5. Overexpression of *StCOMT1* in potato increases resistance to *F. sporotrichioides*

To investigate the role of *StCOMT1* overexpression in potato disease resistance, we verified the function of the *StCOMT1* gene. The results of trypan blue staining showed that with the increase in the duration of *F. sporotrichioides* infection, the area of blue spots on the leaves gradually expanded. On the 7 dai with *F. sporotrichioides*, the blue areas on the leaves of WT were larger compared to those of OE1 and OE2, indicating that the cell death in WT leaves was higher (Fig. 5-A). To investigate the response of the transgenic lines to *F. sporotrichioides* on potato leaves was examined using scanning electron microscopy. Three days after inoculation, *F. sporotrichioides* formed a dense mycelial network on the leaf surface. However, the morphology of some hyphae on the leaves of *StCOMT1*-overexpressing plants showed evidence of shriveling and wilting compared with the WT hyphae (Fig. 5-B).

The results of DAB staining showed that the reddish-brown parts of WT leaves increased days after inoculation, as compared with OE1 and OE2 leaves (Fig. 5-C), indicating that OE lines produced less H_2O_2 than WT under stress, resulting in less damage to the cellular structure. As the infection time with *F. sporotrichioides* increased, the diameters of the leaf lesions expanded. In contrast, except for 0 dai, the diameters of lesions in the OE1 and OE2 were significantly smaller than those in the WT (Fig. 5-D).

To determine whether the level of ROS scavenging was altered in the transgenic plants, we measured H_2O_2, $O_2^{\cdot-}$, CAT, POD, and SOD in WT and OE potato leaves under *F. sporotrichioides*- inoculated and uninoculated conditions over time. The content of H_2O_2 in WT plants was significantly higher than that in OE lines at 0, 1, 3, 5, and 7 dai, and these results were consistent with the DAB staining results (Fig. 5-E). The $O_2^{\cdot-}$ content increased in WT plants at 3 dai, which may be related to immunity signaling (Fig. 5-F). CAT is an important

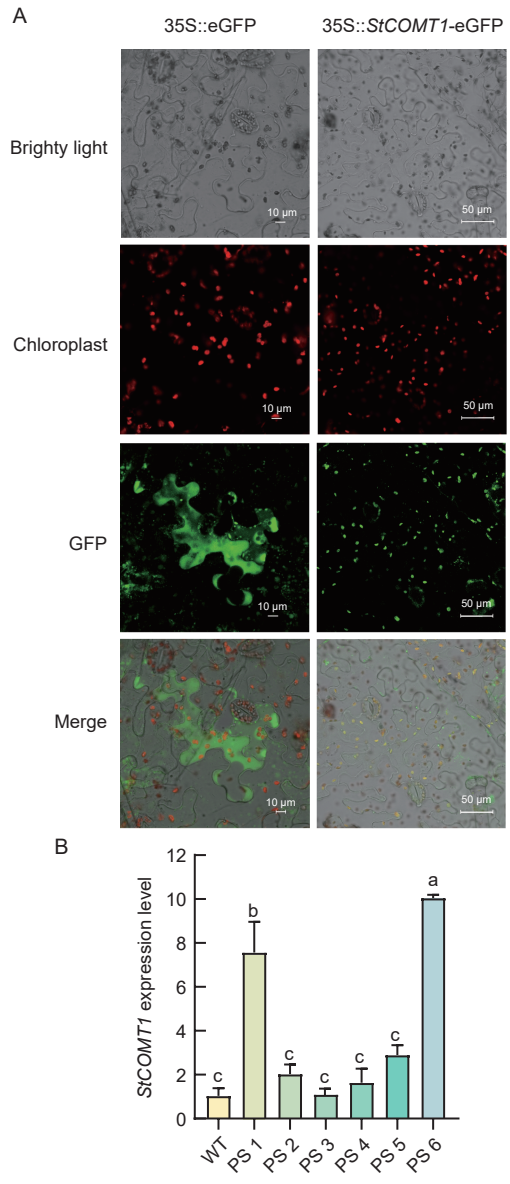


Fig. 4 Subcellular localization of StCOMT1 and acquisition of *StCOMT1* overexpressing potato plants. A, pCambia2300-*StCOMT1*-eGFP localized in chloroplasts while GFP alone localised throughout the cell. From top to bottom, respectively are light field, chloroplast fluorescence signal, GFP fluorescence signal, and superimposed images. B, detection of *StCOMT1* gene expression in transgenic plants PS 1–6. Error bars represent SD (n=3). Different lowercase letters indicate that the differences between treatments were significant at the P<0.01 level.

catalase involved in ROS scavenging. In WT plants, CAT enzyme activity reached the maximum value at 0 dai and decreased with days after infection. The CAT activity of OE1 reached maximum value at 1 dai and then showed a downward trend, while the CAT activity of the OE2 line continued to increase after infection. In general, the CAT activity of the two OE lines was lower than that of the WT plants (Fig. 5-G). After inoculation with *F. sporotrichioides*, the expression levels of POD in WT, OE1 and OE2 fluctuated with time. At 7 dai, the expression level of POD in WT was significantly higher than that in OE1 and OE2 (Fig. 5-H). The SOD enzyme activity of OE1 and OE2 plants was generally lower than that of WT (Fig. 5-I).

3.6. Overexpression of *StCOMT1* resulted in organ-specific accumulation of coumarin-related compounds and organ-specific upregulation of coumarin synthesis genes

Histochemical localization of coumarins in stems, leaves, and tubers of WT and OE plants was determined using laser confocal microscopy. The coumarins could result in blue fluorescence as detectable in the DAPI channel. In tubers, fluorescence was mainly observed in starch grains, and the fluorescence intensity was not significantly altered by the transgene (Fig. 6-A). The blue fluorescence of both WT and OE leaves was distributed in and around the stomata. However, the fluorescence in OE leaves appeared to be enhanced compared to that in WT leaves (Fig. 6-B). In both WT and OE stem segments, blue fluorescence was found in the periderm and xylem. The periderm and xylem of the OE stem segments appeared to have enhanced blue fluorescence as compared with those of WT stems. Additionally, there was a large amount of fluorescence in the lenticels in OE1, indicating increased accumulation of coumarin compared to WT (Fig. 6-C).

Accumulation of melatonin, ferulic acid, caffeic acid, and scopolamine in roots, stems, leaves and tubers of WT, OE1 and OE2 plants without inoculation and with inoculation at 3 d was determined by high-performance liquid chromatography (Fig. 6). In uninoculated plants, the ferulic acid content in the stems of OE1 was much higher than that in the stems of WT. The ferulic acid content in OE1 was 20 times that in WT, and the content of ferulic acid in OE2 was 2.6 times that in WT. However, the content of ferulic acid in the leaves of the two overexpression lines was similar. After inoculation, the ferulic acid content decreased in OE1 and OE2 leaves but increased in WT leaves (Fig. 6-D). The caffeic acid content in OE1 and OE2 potato tubers was significantly higher than in WT tubers and other parts when uninoculated. After inoculation, the caffeic acid content increased in both WT and OE tubers, while the content in leaves decreased (Fig. 6-E). Under uninoculated conditions, scopoletin lactone levels were significantly higher in leaves, stems, and tubers of OE potato plants compared to WT. However, under inoculation conditions, the content of scopolamine lactone in WT, OE1 and OE2 plants decreased in all parts (Fig. 6-F). The melatonin content in the roots and stems of the OE lines was higher than that in the corresponding parts in WT when uninoculated (Fig. 6-G).

Normalization of *StCOMT1* expression showed constitutive expression in all tissues, including roots, stems, leaves, and tubers, after inoculation. Furthermore, it was observed that the *StCOMT1* gene exhibited consistent expression levels in the roots, stems, leaves, and tubers of the WT plants. However, in OE plants, *StCOMT1* displayed significant variability across different tissues. *StCOMT1* expression was highest in OE plant roots, followed by stems, tubers, and then leaves (Fig. 6-H). Based on differences in *StCOMT1* expression across various organs, we investigated the changes in the expression of coumarin-related genes in

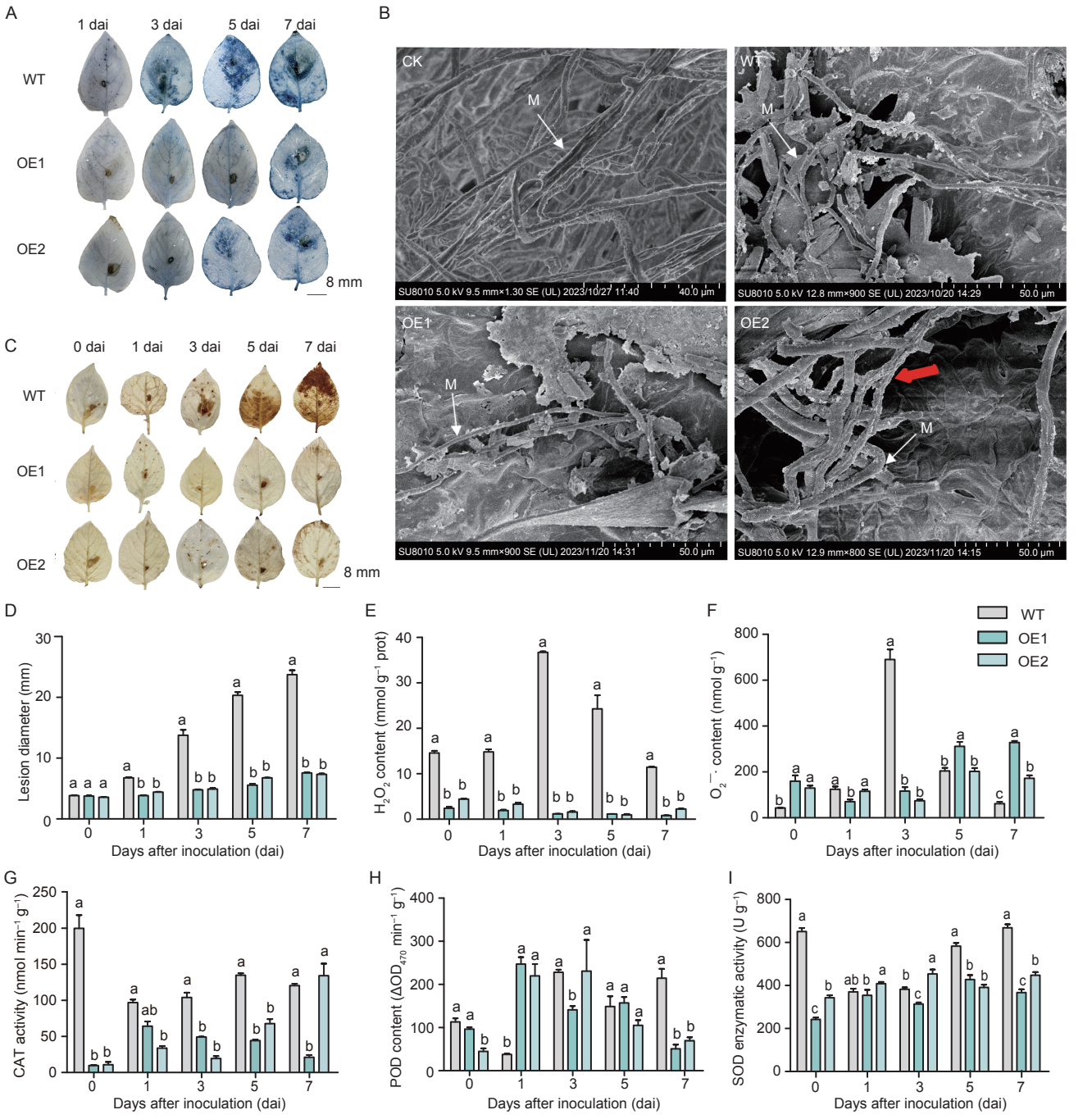


Fig. 5 Responses of potato lines overexpressing *StCOMT1* following infection with *Fusarium sporotrichioides*. A, trypan blue staining results indicated the extent of cell death in OE1, OE2 and WT leaves at 1, 3, 5, and 7 days after inoculation (dai) by *F. sporotrichioides*. B, scanning electron microscopy of fungal colonization on potato leaves: morphology of *F. sporotrichioides* mycelium grown in the petri dish (CK), *F. sporotrichioides* mycelium colonizing the leaf surface of WT plants (WT), *F. sporotrichioides* mycelium colonizing *StCOMT1* OE1 and OE2 potato leaves (OE1 and OE2). M represents hyphae. C, diaminobenzidine staining results of OE1, OE2 and WT leaves at 0, 1, 3, 5, and 7 dai by *F. sporotrichioides*. D, changes in the size of leaf lesions over time post-inoculation. E–I, detection results of H_2O_2, $O_2^{\cdot-}$, catalase (CAT), peroxidase (POD) and superoxide dismutase (SOD) levels in leaves. Error bars represent SD (n=3). Different lowercase letters indicate that the differences between treatments were significant at the P<0.05 level.

different parts. The RT-qPCR results, shown in Fig. 6-I, indicate that *PAL* and *COSY* were highly expressed in roots, stems, and tubers of overexpressed plants compared to the wild type after inoculation. In the transgenic plants, *4CL*, *HCT*, and *UGT* were up-regulated in all parts. Meanwhile, *C4H*, *F6′H*, and *S8H* were highly expressed in leaves, roots, and stems. *CCoAOMT1*, *CYP82C4*, and *BGLU* were highly expressed only in roots and leaves. Finally, *C3′H* was highly expressed in leaves, roots, and tubers. These results indicated that after inoculation the overexpression of *StCOMT1* in potato upregulated coumarin-pathway gene expression and may have led to the accumulation of coumarin-related compounds with organ-specific accumulation.

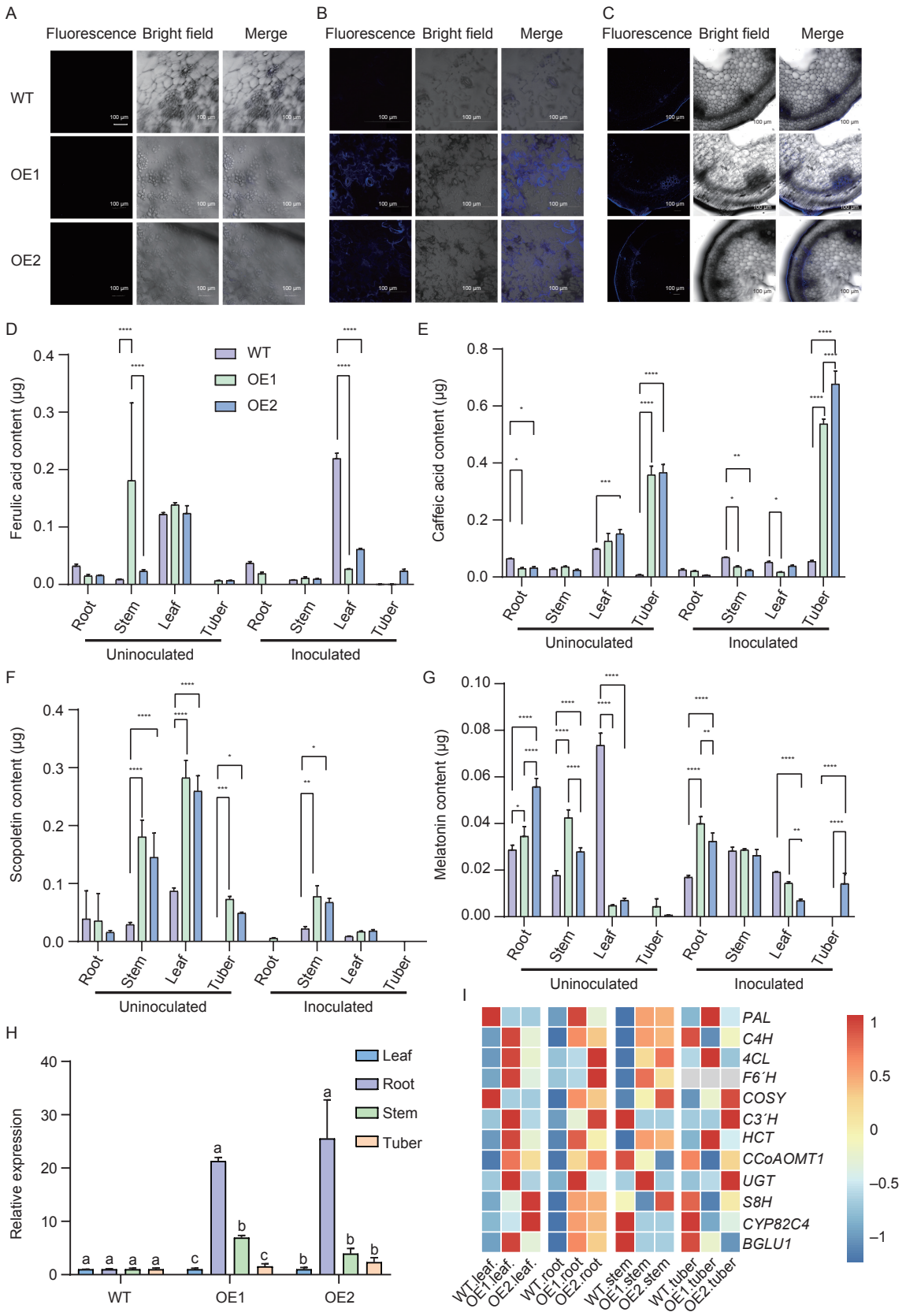


Fig. 6 Tissue specificity of coumarin-related compounds and gene expression. A–C, histochemical localization of coumarins in tubers, leaves, and stems, respectively, of WT and OE1 and OE2 plants. The excitation wavelength is 353 nm, scale bar=100 μm. D–G, the content of ferulic acid, caffeic acid, scopolamine lactone, and melatonin in different tissue sites of WT *vs*. OE1 and OE2, respectively. H, expression of *StCOMT1* in different parts of WT, OE1 and OE2 potato plants. The data of each group were normalized using the *StCOMT1* expression of leaves in WT, OE1, and OE2 as 1, respectively. Error bars represent SD (n=3). *, P<0.05; **, P<0.01; ***, P<0.001; ****, P<0.0001. I, the expression levels of coumarin biosynthesis genes in different organs of the plant.

4. Discussion

COMT is an important methyltransferase in the plant phenylpropanoid metabolic pathway. As a key rate-limiting enzyme, COMT can catalyze the methylation reaction in the synthesis pathway of coumarin and lignin, which are important secondary metabolites, thus playing a crucial role in these pathways. These secondary metabolites play an important role in plant morphogenesis and defense response. The *COMT* gene family has been identified in several species, but it has not yet been reported in the 'Atlantic' potato. Previous studies have shown that the number of *COMT* gene family members varies among different species. For instance, *Vaccinium uliginosum* has 92 *COMT* genes, *Brassica napus* has 42 *COMT* genes, and *Glycine max* has 55 *COMT* genes (Li *et al.* 2016; Liu *et al.* 2021; Zhang *et al.* 2021). A total of 123 *StCOMTs* were identified in 'Atlantic' potato, but they were not evenly distributed across all chromosomes. Instead, they were densely concentrated in specific chromosomal regions (Fig. 1-D). This may be due to frequent local crosstalk or proximal gene duplication (Lu *et al.* 2022). The Ka/Ks ratios of all duplicated gene pairs in the *StCOMT* gene family were less than 1, suggesting that the potato *COMT* genes underwent purifying selection during the evolutionary process (Duan *et al.* 2024). This pattern of gene duplication has also been observed in other studies on *COMT* from *Vitis vinifera* L., *Actinidia chinensis* Planch., *Rhododendron williamsianum* Rehder & E. H. Wilson, and *V. uliginosum* (Liu *et al.* 2021).

COMT is capable of recognising various substrates and catalyzing different catechol-containing compounds (Wang Q *et al.* 2018). Previous *in vitro* enzyme activity experiments have shown that COMT catalyzes the methylation of caffeoyl- and 5-hydroxyferuloyl-containing alcohols, aldehydes, and acids, with a kinetic preference for alcohols and aldehydes over free acids (Zubieta *et al.* 2002). Additionally, COMT displays higher catalytic affinity and specificity for quercetin (Zubieta *et al.* 2002). The difference in catalytic activity between the reaction of AtCOMT towards caffeic acid and N-acetyl-5-hydroxytryptamine is believed to be due to the structural limitations of N-acetyl-5-hydroxytryptamine in binding to AtCOMT (Wang *et al.* 2019). Validating the *in vitro* enzymatic activity of StCOMT1 can provide fundamental support for subsequent physicochemical mutation of the protein. This can improve substrate affinity and increase the catalytic activity and specificity of StCOMT1 towards the substrate, reducing metabolic loss in the pathway.

Fusarium sporotrichioides is a common soil-borne pathogen causing potato dry rot in northeast China (Jiang *et al.* 2017) *COMT* has been reported to be involved in lignin biosynthesis and functions as a defense-associated protein that is strongly responsive during pathogen infection and elicitor treatment (Yang *et al.* 2024). The *AtCOMT1* mutant has been found to be more susceptible to two necrotrophic fungi, one biotrophic fungus and two bacterial pathogens (Quentin *et al.* 2009). Potato leaves overexpressing the *StCOMT1* transgenic lines used in this experiment showed a significant increase in disease resistance compared to WT after *F. sporotrichioides* infestation, with marked reduction in of leaf damage. The excessive accumulation of H_2O_2 leads to oxidative damage, thereby causing lesions. Overexpression of *StCOMT1* is associated with reduced H_2O_2 and $O_2^{-}\cdot$ content, which could reduce oxidative damage. The accumulation of coumarin-related compounds such as melatonin, ferulic acid, caffeic acid and scopolamine, has been implicated in plant resistance to pathogenic fungi (Gao *et al.* 2024; Liu *et al.* 2024). The reduction of oxidative damage by overexpression of *StCOMT1* may be related to the accumulation of bioactive compounds such as melatonin. Several studies have shown that the melatonin can induce plant resistance to biotic stress by activating antioxidant defense (Li *et al.* 2012; Ahammed *et al.* 2024; Chen *et al.* 2025). It was previously shown that dwarfing was significantly alleviated in melatonin-enriched tomato plants, where melatonin accumulation effectively limited ROS production, mitigating stress by triggering antioxidant enzyme activities (especially CAT and APX) or scavenging H_2O_2 (Zhang *et al.* 2022). In the current study, the overexpression of *StCOMT1* in potato leaves appeared to affect the morphology of colonized *F. sporotrichioides* growing upon those leaves. Chaetoglobosin A has been shown to inhibit the mycelial growth of *F. sporotrichioides* (Jiang *et al.* 2017). In a previous study, thymol and SA induced mycelial crumpling of *F. solani*, which was found to disrupt the integrity and permeability of the cell membrane and even hinder mitochondrial function. As a result, this led to the inhibition of *F. solani* activity and even death (Kong *et al.* 2021). Previous studies have shown that the coumarin analogue scopoletin has been found to have an inhibitory effect on the assembly of *F. oxysporum* colonies (Stringlis *et al.* 2018). In the current study, overexpression of *StCOMT1* was associated with the accumulation of the coumarin compound scopoletin (Fig. 6-F). In this study, mycelial morphology appeared to be altered (Fig. 5-B), and *StCOMT1* overexpression plants were less stressed by *F. sporotrichioides* (Fig. 5-A). This might be because the overexpression of *StCOMT1* inhibits the growth of fungi through regulatory mechanisms such as increased the synthesis of caffeic acid and ferulic acid, thereby affecting the interaction between plants and *F. sporotrichioides* (Ferruz *et al.* 2016). Previous studies in *A. thaliana* have shown that the down-regulation of *COMT* expression can drastically alter the interaction between a plant and biotic environment (Quentin *et al.* 2009). In addition, *COMT* is associated with the biosynthesis of metabolites such as lignin, flavonoids, and stilbenes (Lam *et al.* 2024). The overexpression of *COMT* usually leads to alterations in lignin composition, the composition of cell wall-bound substances, and soluble phenolics (Funnell-Harris *et al.* 2023). In resistant sorghum, sinapaldehyde, which is catalyzed by the COMT enzyme encoded by *Bmr12*, exhibits antibacterial properties (Wang *et al.* 2025). A systematic analysis indicates that *VvCOMT1* may play a role in the synthesis of most methylated flavonoids in grape berry skin (Lu *et al.* 2022). The flavonoid pathway and the phenylpropanoid pathway are crucial for plant defense (Jiang *et al.* 2025). Moreover, resistance mediated by *COMT* against the polyphagous insect pest fall armyworm (FAW; *Spodoptera frugiperda*) in sorghum largely depends on JA (Kundu *et al.* 2025). Therefore, whether the

overexpression of *StCOMT1* enhances the disease resistance of potatoes by influencing the synthesis of other secondary metabolites and hormones is worth further investigation.

The overexpression of *StCOMT1* resulted in distinct changes in coumarin analogues and pathway genes across various organs. In cassava treated with MeJA, coumarins were shown to exhibit tissue-specific distribution, and the *OMT* genes responsible for their biosynthesis displayed tissue-specific and induced expression specificity (He *et al.* 2023). In the current study, the overexpression of *StCOMT1* led to a significant increase in scopolamine content in potato leaves. Overexpression of *StCOMT1* caused the accumulation of caffeic acid and other bioactive compounds, which have been shown to play a role in disease resistance in some other plants. Scopolamine has been shown to have antifungal activity against *Phakopsora pachyrhizi*, the fungus that causes Asian soybean rust, and inhibits the germination of the pathogen's spores, thus protecting soybeans from infection (Beyer *et al.* 2019). RNAi interference of *COMT* expression in barley did not systematically alter ferulic acid content (Daly *et al.* 2018), and overexpression of *StCOMT1* also had a minor effect on ferulic acid content in this study. Different plant organs have different degrees of response to pathogens and have different defense measures (Smakowska *et al.* 2016; Lacaze and Joly 2020). We speculated that the organizational differences in coumarin pathway gene expression and contents of coumarin-related compounds induced by overexpression of *StCOMT1* might be related to the organ-specific defense mechanisms in different plant organs. Organ and tissue specificity of antimicrobial compounds in other Solanaceous plants has also been observed (Lacaze and Joly 2020). Changes of gene expression in the phenylpropanoid metabolic pathway may redirect metabolic flux in this pathway, thereby playing a role in disease resistance (Hu *et al.* 2018; Xiao *et al*. 2021). As a key gene for lignin and coumarin synthesis, whether overexpression of *StCOMT1* can mediate resistance to *F. sporotrichioides* by enhancing catalytic methylation and thereby redirecting the metabolic flux within the phenylpropanoid pathway of potato between the lignin and coumarin synthesis pathways remains to be further investigated.

5. Conclusion

Overexpression of *StCOMT1* may increase resistance of potato to *F. sporotrichioides*. In this study, the potato *COMT* gene family was identified, which provides valuable information for further research on the evolution and gene function of the *COMT* gene family in potato. Combined with the previous analysis of potato transcriptional metabolism induced by DON, *StCOMT1* was screened as a gene involved in secondary metabolism and shown to play an important role in potato disease resistance. Overexpression of *StCOMT1* in potato can promote the up-regulation of coumarin synthesis-related genes such as *StPAL*, *StCCoAOMT1*, and *StCYP82C4*, leading to the organ-specific accumulation of coumarin-related secondary metabolites such as melatonin and scopolamine, affect the mycelial morphology of *F. sporotrichioides* and remove ROS. Thus, the disease resistance of potato to *F. sporotrichioides* was improved.

Acknowledgements

This work was supported by the National Natural Science Foundation of China (U22A20443); the Heilongjiang Provincial Research Institutes Scientific Research Operating Expenses Project, China (CZKYF2023-1-B020); the Key Research and Development Plan Project of Heilongjiang Province, China (GA23B015) and the Young Scientists Fund of the National Natural Science Foundation of China (32201717).

Declaration of competing interest

The authors declare that they have no conflict of interest.

Declaration of generative AI and AI-assisted technologies in the writing process

The authors declare that they did not use AI in the preparation and writing of this manuscript.

Data availability

The RNA-seq datasets in this study are available from the NCBI Sequence Read Archive under project PRJNA943451.

Appendices associated with this paper are available at https://doi.org/10.1016/j.jia.2025.11.021

References

Ahammed G J, Li Z, Chen J, Dong Y, Qu K, Guo T, Wang F, Liu A, Chen S, Li X. 2024. Reactive oxygen species signaling in melatonin-mediated plant stress response. *Plant Physiology and Biochemistry*, **207**, 108398.

Beyer S F, Beesley A, Rohmann P F W, Schultheiss H, Conrath U, Langenbach C J G. 2019. The Arabidopsis non-host defence-associated coumarin scopoletin protects soybean from Asian soybean rust. *The Plant Journal*, **99**, 397–413.

Bruce M A, Shoup Rupp J L. 2019. *Agrobacterium*-mediated transformation of *Solanum tuberosum* L., potato. *Methods in Molecular Biology* (Clifton, N.J.), **1864**, 203–223.

Camire M E, Kubow S, Donnelly D J. 2009. Potatoes and human health. *Critical Reviews in Food Science and Nutrition*, **49**, 823–840.

Cannon S B, Mitra A, Baumgarten A, Young N D, May G. 2004. The roles of segmental and tandem gene duplication in the evolution of large gene families in *Arabidopsis thaliana*. *BMC Plant Biology*, **4**, 10.

Chang J J, Guo Y L, Yan J Y, Zhang Z X, Yuan L, Wei C H, Zhang Y, Ma J X, Yang J Q, Zhang X, Li H. 2021. The role of watermelon caffeic acid *O*-methyltransferase (*ClCOMT1*) in melatonin biosynthesis and abiotic stress tolerance. *Horticulture Research*, **8**, 210.

Chao J T, Kong Y Z, Wang Q, Sun Y H, Gong D P, Lv J, Liu G S. 2015. MapGene2Chrom, a tool to draw gene physical map based on Perl and SVG languages. *Hereditas*, **37**, 91–97. (in Chinese)

Chen C J, Chen H, Zhang Y, Thomas H R, Frank M H, He Y, Xia R. 2020. TBtools: An integrative toolkit developed for interactive analyses of big biological data. *Molecular Plant*, **13**, 1194–1202.

Chen Q, Chen Y, Li X, Zhang L, Rengel Z. 2025. Phytomelatonin: Biosynthesis, signaling, and functions. *Annual Review of Plant Biology*, **76**, 171–195.

Daly P, McClellan C, Maluk M, Oakey H, Lapierre C, Waugh R, Stephens J, Marshall D, Barakate A, Tsuji Y, Goeminne G, Vanholme R, Boerjan W, Ralph J, Halpin C. 2018. RNAi-suppression of barley caffeic acid *O*-methyltransferase modifies lignin despite redundancy in the gene family. *Plant Biotechnology Journal*, **17**, 594–607.

Daudi A, O'Brien J A. 2012. Detection of hydrogen peroxide by DAB staining in *Arabidopsis* leaves. *Bio-Protocol*, **2**, e263.

Doppler M, Kluger B, Bueschl C, Steiner B, Buerstmayr H, Lemmens

M, Krska R, Adam G, Schuhmacher R. 2019. Stable isotope-assisted plant metabolomics: Investigation of phenylalanine-related metabolic response in wheat upon treatment with the *Fusarium* virulence factor deoxynivalenol. *Frontiers in Plant Science*, **10**, 1137.

Duan S F, Yu J C, Baldwin T C, Yuan Y, Xiang G S, Cui R, Zhao Y, Mo X C, Lu Y C, Liang Y L. 2024. Genome-wide identification of a MADS-box transcription factor family and their expression during floral development in *Coptis teeta* wall. *BMC Plant Biology*, **24**, 1023.

Fan Y L, Zhang W N, Kang Y C, Shi M F, Yang X Y, Yu H F, Zhang R Y, Liu YH, Qin S H. 2021. Physiological and dynamic transcriptome analysis of two potato varieties reveal response of lignin and MAPK signal to dry rot caused by *Fusarium sulphureum*. *Scientia Horticulturae*, **289**, 110470.

Feng Y M, Qi P Y, Xiao W L, Zhang T H, Zhou X, Liu L W, Yang S. 2022. Fabrication of isopropanolamine-decorated coumarin derivatives as novel quorum sensing inhibitors to suppress plant bacterial disease. *Journal of Agricultural and Food Chemistry*, **70**, 6037–6049.

Ferruz E, Atanasova-Pénichon V, Bonnin-Verdal M N, Marchegay G, Pinson-Gadais L, Ducos C, Lorán S, Ariño A, Barreau C, Richard-Forget F. 2016. Effects of phenolic acids on the growth and production of T-2 and HT-2 toxins by *Fusarium langsethiae* and *F. sporotrichioides*. *Molecules* (Basel, Switzerland), **21**, 449.

Funnell-Harris D, Sattler S, O'Neill P, Gries T, Ge Z, Nersesian N. 2023. Effects of altering three steps of monolignol biosynthesis on sorghum responses to stalk pathogens and water deficit. *Plant Disease*, **107**, 3984–3995.

Gao L Y, Wang P, Yan X, Li J M, Ma L, Hu M H, Ge X Y, Li F G, Hou Y X. 2024. Feruloyl-CoA 6´-hydroxylase-mediated scopoletin accumulation enhances cotton resistance to *Verticillium dahliae*. *Plant Physiology*, **196**, 3007–3022.

He Y D, Zhang J, He Y W, Liu H H, Wang C, Guan G P, Zhao Y C, Tian Y, Zhong X H, Lu X Y. 2023. Two *O*-methyltransferases are responsible for multiple *O*-methylation steps in the biosynthesis of furanocoumarins from *Angelica decursiva*. *Plant Physiology and Biochemistry*, **204**, 108142.

Hu Q, Min L, Yang X Y, Jin S X, Zhang L, Li Y Y, Ma Y Z, Qi X W, Li D Q, Liu H B, Lindsey K, Zhu L F, Zhang X L. 2018. Laccase GhLac1 modulates broad-spectrum biotic stress tolerance via manipulating phenylpropanoid pathway and jasmonic acid synthesis. *Plant Physiology*, **176**, 1808–1823.

Jiang C, Song J Z, Zhang J Z, Yang Q. 2017. Identification and characterization of the major antifungal substance against *Fusarium sporotrichioides* from *Chaetomium globosum*. *World Journal of Microbiology & Biotechnology*, **33**, 1–9.

Jiang T, Hao T W, Chen W J, Li CL, Pang S Q, Fu C L, Cheng J, Zhang C B, Ghorbanpour M, Miao S. 2025. Reprogrammed plant metabolism during viral infections: mechanisms, pathways and implications. *Molecular Plant Pathology*, **26**, e70066.

Kong J, Xie Y F, Yu H, Guo Y H, Cheng Y L, Qian H, Yao W R. 2021. Synergistic antifungal mechanism of thymol and salicylic acid on *Fusarium solani*. *LWT-Food Science and Technology*, **140**, 110787.

Kundu P, Shinde S, Grover S, Sattler S, Louis J. 2025. Caffeic acid *O*-methyltransferase-dependent flavonoid defenses promote sorghum resistance to fall armyworm infestation. *Plant Physiology*, **197**, kiaf071.

Lacaze A, Joly D L. 2020. Structural specificity in plant–filamentous pathogen interactions. *Molecular Plant Pathology*, **21**, 1513–1525.

Lam L, Lui A, Bartley L, Mikami B, Umezawa T, Lo C. 2024. Multifunctional 5-hydroxyconiferaldehyde *O*-methyltransferases (CAldOMTs) in plant metabolism. *Journal of Experimental Botany*, **75**, 1671–1695.

Letunic I, Bork P. 2007. Interactive tree of life (iTOL): An online tool for phylogenetic tree display and annotation. *Bioinformatics*, **23**, 127–128.

Li C, Wang P, Wei Z W, Liang D, Liu C H, Yin L H, Jia D F, Fu M Y, Ma F W. 2012. The mitigation effects of exogenous melatonin on salinity-induced stress in *Malus hupehensis*. *Journal of Pineal Research*, **53**, 298–306.

Li L, Wang S C, Yang X F, Francis F, Qiu D W. 2019. Protein elicitor PeaT1 enhanced resistance against aphid (*Sitobion avenae*) in wheat. *Pest Management Science*, **76**, 236–243.

Li W, Lu J X, Lu K, Yuan J L, Huang J H, Du H, Li J. 2016. Cloning and phylogenetic analysis of *Brassica napus* L. caffeic acid *O*-methyltransferase 1 gene family and its expression pattern under drought stress. *PLoS ONE*, **11**, e0165975.

Li Z, Zhang Y, Ren J, Jia F L, Zeng H M, Li G Y, Yang X F. 2022. Ethylene-responsive factor ERF114 mediates fungal pathogen effector PevD1-induced disease resistance in *Arabidopsis thaliana*. *Molecular Plant Pathology*, **23**, 819–831.

Liang S M, Xu S B, Qu D, Yang L M, Wang J G, Liu H L, Xin W, Zou D T, Zheng H L. 2022. Identification and functional analysis of the caffeic acid O-methyltransferase (COMT) gene family in rice (*Oryza sativa* L.). *International Journal of Molecular Sciences*, **23**, 8491.

Liu H B, Wang Y R, Chang Q Z, Li Q B, Fang J H, Cao N, Tong X J, Jiang X M, Yu X H, Cheng Y. 2024. Combined metabolome and transcriptome reveal *HmF6´H1* regulating simple coumarin accumulation against powdery mildew infection in *Heracleum moellendorffii* Hance. *BMC Plant Biology*, **24**, 507.

Liu J X, Wang P Y, Wang Y F, Zhang Y J, Xu T Q, Zhang Y Q, Xi J, Hou L J, Li L, Zhang Z Q, Lin Y B. 2022. Negative effects of poly (butylene adipate-co-terephthalate) microplastics on *Arabidopsis* and its root-associated microbiome. *Journal of Hazardous Materials*, **437**, 129294.

Liu Y S, Wang Y Z, Pei J B, Li Y D, Sun H Y. 2021. Genome-wide identification and characterization of *COMT* gene family during the development of blueberry fruit. *BMC Plant Biology*, **21**, 5.

Lu S W, Zhuge Y X, Hao T Y, Liu Z J, Zhang M W, Fang J G. 2022. Systematic analysis reveals *O*-methyltransferase gene family members involved in flavonoid biosynthesis in grape. *Plant Physiology and Biochemistry*, **173**, 33–45.

Ma L, Jiang H, Ren Y Y, Yang J W, Han Y, Si H J, Prusky D, Bi Y, Wang Y. 2022. Overexpression of *StCDPK23* promotes wound healing of potato tubers by regulating *StRbohs*. *Plant Physiology and Biochemistry*, **185**, 279–289.

Ma Q H, Xu Y, Lin Z B, He P. 2002. Cloning of cDNA encoding *COMT* from wheat which is differentially expressed in lodging-sensitive and -resistant cultivars. *Journal of Experimental Botany*, **53**, 2281–2282.

Morimura H, Ito M, Yoshida S, Koitabashi M, Tsushima S, Camagna M, Chiba S, Takemoto D, Kawakita K, Sato I. 2020. *In vitro* assessment of biocontrol effects on *Fusarium* head blight and deoxynivalenol (DON) accumulation by DON-degrading bacteria. *Toxins*, **12**, 399.

Pasare S A, Ducreux L J M, Morris W L, Campbell R, Sharma S K, Roumeliotis E, Kohlen W, van der Krol S, Bramley P M, Roberts A G, Fraser P D, Taylor M A. 2013. The role of the potato (*Solanum tuberosum*) *CCD8* gene in stolon and tuber development. *The New Phytologist*, **198**, 1108–1120.

Quentin M, Allasia V, Pegard A, Allais F, Ducrot P H, Favery B, Levis C, Martinet S, Masur C, Ponchet M, Roby D, Schlaich N L, Jouanin L, Keller H. 2009. Imbalanced lignin biosynthesis promotes the sexual reproduction of homothallic oomycete pathogens. *PLoS Pathogens*, **5**, e1000264.

Saluja M, Zhu F, Yu H, Walia H, Sattler S E. 2020. Loss of COMT activity reduces lateral root formation and alters the response to water limitation in sorghum *brown midrib* (*bmr*) *12* mutant. *New Phytologist*, **229**, 2780–2794.

Seong E S, Yoo J H, Lee J G, Kim H Y, Hwang I S, Heo K, Kim J K, Lim J D, Sacks E J, Yu C Y. 2012. Antisense-overexpression of the *MsCOMT* gene induces changes in lignin and total phenol contents in transgenic tobacco plants. *Molecular Biology Reports*, **40**, 1979–1986.

Smakowska E, Kong J, Busch W, Belkhadir Y. 2016. Organ-specific regulation of growth-defense tradeoffs by plants. *Current Opinion in Plant Biology*, **29**, 129–137.

Stokstad E. 2019. The new potato. *Science*, **363**, 574–577.

Stringlis I A, Yu K, Feussner K, de Jonge R, Van Bentum S, Van Verk M C, Berendsen R L, Bakker P A H M, Feussner I, Pieterse C M J. 2018. MYB72-dependent coumarin exudation shapes root microbiome assembly to promote plant health. *Proceedings of the National Academy of Sciences of the United States of America*, **115**, E5213–E5222.

Tiwari R K, Lal M K, Kumar R, Sharma S, Sagar V, Kumar A, Singh B, Aggarwal R. 2023. Impact of *Fusarium* infection on potato quality, starch digestibility, *in vitro* glycemic response, and resistant starch content. *Journal of Fungi*, **9**, 466.

Wang M X, Zhu X L, Wang K, Lu C G, Luo M Y, Shan T L, Zhang Z Y. 2018. A wheat caffeic acid 3-*O*-methyltransferase *TaCOMT-3D* positively contributes to both resistance to sharp eyespot disease

and stem mechanical strength. *Scientific Reports*, **8**, 6543.
Wang Q, Teng M K, Li X. 2018. Functional and structural characterization of a novel catechol-*O*-methyltransferase from *Schizosaccharomyces pombe*. *IUBMB Life*, **71**, 330–339.
Wang Q, Veley K, Johnson J, Sumner J, van Erven G, Kabel M, Dhungana S, Berry J, Boyher A, Braun D, Vermerris W, Bart R. 2025. Three *Xanthomonas* cell wall degrading enzymes and sorghum *Brown midrib 12* contribute to virulence and resistance in the bacterial leaf streak pathosystem. *Molecular Plant–Microbe Interactions*, **38**, 400–410.
Wang W Y, Su S S, Wang S Z, Ye L D, Yu H W. 2019. Significantly improved catalytic efficiency of caffeic acid *O*-methyltransferase towards N-acetylserotonin by strengthening its interactions with the unnatural substrate's terminal structure. *Enzyme and Microbial Technology*, **125**, 1–5.
Wang Y P, Tang H B, DeBarry J D, Tan X, Li J P, Wang X Y, Lee T H, Jin H Z, Marler B, Guo H, Kissinger J C, Paterson A H. 2012. MCScanX: A toolkit for detection and evolutionary analysis of gene synteny and collinearity. *Nucleic Acids Research*, **40**, e49.
van Wees S. 2008. Phenotypic analysis of *Arabidopsis* mutants: Trypan blue stain for fungi, oomycetes, and dead plant cells. *CSH Protocols*, doi: 10.1101/pdb.prot4982.
Wei X H, Feng X, He F M, Xu Y Q, Li J Y, Xiao M M, Li L, Li C T, Yuan Q, Li F L. 2023. Efficacy of vomitoxin as elicitor for controlling soilborne diseases on potato plants. *Journal of Fujian Agricultural Sciences*, **38**, 329–338. (in Chinese)
Xiao S H, Hu Q, Shen J L, Liu S M, Yang Z G, Chen K, Klosterman S J, Javornik B, Zhang X L, Zhu L F. 2021. *GhMYB4* downregulates lignin biosynthesis and enhances cotton resistance to *Verticillium dahliae*. *Plant Cell Reports*, **40**, 735–751.
Xue H L, Bi Y, Wei J M, Tang Y M, Zhao Y, Wang Y. 2013. New method for the simultaneous analysis of types A and B trichothecenes by ultrahigh-performance liquid chromatography coupled with tandem mass spectrometry in potato tubers inoculated with *Fusarium sulphureum*. *Journal of Agricultural and Food Chemistry*, **61**, 9333–9338.
Xue H L, Bi Y, Zong Y Y, Alejandro C, Wang H J, Pu L M, Wang Y, Li Y C. 2017. Effects of elicitors on trichothecene accumulation and *Tri* genes expression in potato tubers inoculated with *Fusarium sulphureum*. *European Journal of Plant Pathology*, **148**, 673–685.
Xue H L, Liu Q L, Yang Z M. 2023. Pathogenicity, mycotoxin production, and control of potato dry rot caused by *Fusarium spp*.: A Review. *Journal of Fungi*, **9**, 843.
Yang C, Wang X J, Li S W, Zhu X R, Yu Y W, Zhang S Y. 2024. Combined analysis of transcriptomics with metabolomics provides insights into the resistance mechanism in winter jujube using L-methionine. *Plant Physiology and Biochemistry*, **214**, 108951.
Zhang T, Wang Y, Ma X J, Ouyang Z P, Deng L, Shen S S, Dong X X, Du N S, Dong H, Guo Z H, Meng G, Piao F Z, Sun K L. 2022. Melatonin alleviates copper toxicity via improving ROS metabolism and antioxidant defense response in tomato seedlings. *Antioxidants*, **11**, 758.
Zhang X, Chen B W, Wang L S, Ali S, Guo Y L, Liu J X, Wang J, Xie L N, Zhang Q Z. 2021. Genome-wide identification and characterization of *caffeic acid O-methyltransferase* gene family in soybean. *Plants*, **10**, 2816.
Zhao B, Yu H, Liu D, Wang J Q, Feng X, He F M, Qi T S, Du C, Wang L L, Wang H F, Li F L. 2023. Combined transcriptome and metabolome analysis reveals adaptive defense responses to DON induction in potato. *International Journal of Molecular Sciences*, **24**, 8054.
Zhao D K, Yao Z P, Zhang J M, Zhang R J, Mou Z M, Zhang X, Li Z H, Feng X L, Chen S Y, Reiter R J. 2021. Melatonin synthesis genes N-acetylserotonin methyltransferases evolved into caffeic acid *O*-methyltransferases and both assisted in plant terrestrialization. *Journal of Pineal Research*, **71**, e12737.
Zhao X C, Xu Y Q, He F M, Sun M L, Yuan Q, Wang X, Kong D X, Liu D, Feng Y Z, Chen H S, Tian M, Liu D, Li F L. 2020. Low concentration of vomitoxin as elicitor induced resistance of dry rot disease of potato and its mechanism. *Acta Agronomica Sinica*, **46**, 1801–1809. (in Chinese)
Zöngür A. 2024. Efficacy of *Beta vulgaris* essential oils against potato dry rot disease and deoxynivalenol (DON) mycotoxin. *Potato Research*, **68**, 355–365.
Zubieta C, Kota P, Ferrer J L, Dixon R A, Noel J P. 2002. Structural basis for the modulation of lignin monomer methylation by caffeic acid/5-hydroxyferulic acid 3/5-*O*-methyltransferase. *The Plant Cell*, **14**, 1265–1277.
Zuckerkandl E, Pauling L B. 1965. Evolutionary divergence and convergence in proteins. *Evolving Genes and Proteins*, **1965**, 97–166.
Zuo D Y, Yi S Y, Liu R J, Qu B, Huang T, He W J, Li C, Li H P, Liao Y C. 2016. A deoxynivalenol-activated methionyl-tRNA synthetase gene from wheat encodes a nuclear localized protein and protects plants against *Fusarium* pathogens and mycotoxins. *Phytopathology*, **106**, 614–623.

Executive Editor-in-Chief Sanwen Huang
Managing Editor Lingyun Weng